DOI: 10.1007/s12541-014-0440-8

Micro-Cutting with Diamond Tool Micro-Patterned by Femtosecond Laser

Jaegu Kim[1,#], Tae-Jin Je[1], Sung-Hak Cho[1], Eun-Chae Jeon[1], and Kyung-Hyun Whang[1]

1 Korea Institute of Machinery & Materials, 156, Gajeongbuk-Ro, Yuseong-Gu, Daejeon, South Korea, 305-343
Corresponding Author / E-mail: gugu99@kimm.re.kr, TEL: +82-42-868-7141, FAX: +82-42-868-7149

KEYWORDS: Micro-cutting, Micro-pattern, Diamond machining, Femtosecond laser

The demand for micro-scale surface machining has been steadily increasing, and various methods have been introduced. Among these, microcutting with a diamond tool removes material by making multiple cutting passes. However, many passes are needed to generate micropatterns over a large area. To overcome the drawbacks of this time-consuming process, we propose a novel method, which uses a micropatterned diamond tool. A 220-fs-pulsed Ti: Sapphire laser is used to create micropatterns on the edge line of a rectangular diamond tool. A six-axis motion stage is used to align the edge line and flank surface of the diamond tool with respect to the focal point of the laser beam. Using a simple laser direct-writing method and a 100× objective lens (NA: 0.8), lines ≤2 μm in width, 20 μm in length, and 10 μm in separation were fabricated along the 1-mm edge line of a bulk diamond tool. The micropatterned diamond cutting tool was then used to successfully produce micropatterns on the surface of nickel (Ni)-electroformed on SKD-61. This novel process provides an efficient means of multiple micropattern generation for molding applications, such as those required for optics and biotechnology, using only a single pass of a diamond cutting tool.

Manuscript received: April 15, 2013 / Revised: January 27, 2014 / Accepted: April 17, 2014

1. Introduction

Surface texturing with micro- and nanometer feature sizes is an important technology for improving inherent functions, such as light emission in light-emitting diodes (LEDs),[1] light trapping in photovoltaics,[2] friction force reduction in aerodynamics and tribology,[3,4] and cell proliferation or prevention (or self-cleaning) in bioindustry.[5,6] Bruzzone et al. described the functional properties of surface applications and surface engineering technologies in detail.[7]

The many methods available for micro-fabrication and processing technology are tailored to the specific applications and materials used. From a manufacturing perspective, it is important to balance machining quality and production cost in the fabrication of micropatterns over relatively large areas. Among these methods, diamond cutting is capable of producing submicron features via diamond turning, milling, drilling, and chiseling, with minimal surface roughness (on the order of a few nanometers).[8] However, the shape and area of the machined part are entirely dependent on the shape of the diamond tool. A diamond-cut machined pattern usually requires multiple passes to cover large areas.

The femtosecond laser is a suitable tool for micromachining because the interaction time between the laser beam and the material is too short to generate heat or melting of the material. Mao et al. introduced an overview of the fundamental physics that the femtosecond laser micromachining in dielectric materials, such as natural diamond, results from laser-induced electronic excitation and relaxation, ionizing a large number of electrons, which leads to material ablation.[9] Gattass and Mazur also reviewed the physical mechanisms and described the important emerging applications in transparent materials.[10] They explained unique advantages in favour of femtosecond laser micromachining of transparent materials over other photonic-device fabrication techniques. Many researchers have reported on the machining of diamond by using femtosecond laser irradiation inside the diamond bulk and on the diamond surface to analyze machining characteristics such as submicrometer periodic linear grooves[11] and nanoscale surface structures.[12] For micro texturing to large area, Pettersson and Jacobson presented the embossing tools with well-defined textured diamond surfaces by a photolithographic process.[13] Kuang et al. demonstrated the femtosecond laser surface micro-structuring using a spatial light modulator and galvo scanner.[14] Even though other many microfabrication methods were introduced, each method has pros and cons in terms of pattern shapes, surface qualities, substrate materials and machining time. Therefore, manufactures are

always looking for the process to fabricate micro feature size in large area.

In this paper, we demonstrate an efficient micromachining method that uses the patterned edge of a diamond cutting tool, a few microns in width, to fabricate multiple patterns on metals in a single cutting pass. A 220-fs-pulsed Ti: sapphire laser was used to create micropatterns on the 1-mm edge of a rectangular bulk diamond tool. The micropatterned diamond cutting tool was then used to successfully produce micropatterns in a Ni layer, electroformed on SKD-61.

2. Experiment

2.1 Femtosecond laser machining of bulk diamond

In this study, we used a single-crystal diamond tool, made from natural diamond. The tool had a thickness of 0.5 mm, cutting width of 1 mm, rake angle of 0°, and clearance angle of 3°. To pattern multiple lines along the cutting edge, the flank face of the diamond tool was positioned normal to the incident laser beam, and the edge line was positioned coincident with the direction of stage motion. A six-axis tool holder was used to position the flank face of the diamond tool at the focal point. To position the flank face normal to the laser beam, 3 different position of the flank face were measured. The values of XYZ of each position were used to calculate the normal vector of the flank face and then the value of pitching and rolling were obtained by comparing the normal vector to the direction vector of the laser beam which was propagated only in the z direction.

The flank surface was irradiated by a 220-fs-pulsed Ti: sapphire laser (wavelength: 800 nm; repetition rate: 100 kHz). The beam was focused using a high numerical aperture (NA) lens (NA: 0.8), which produced a 1.2-μm focal spot on the diamond surface.

We determined that ablation occurred for a laser pulse energy of 13 nJ, corresponding to a sample translation speed of 0.01 mm s^{-1}. No surface changes were observed for 6 nJ (the next energy step of our optics system), using the same sample translation speed. Therefore, the irradiation energy was set to 13 nJ to minimize the shock power. Three translation speeds were used to create the pattern in the diamond: 0.01, 0.05, and 0.1 mm s^{-1}. The reciprocating number for a line was 1, 2, and 5 for speeds of 0.01 and 0.05 mm s^{-1}, and 10, 20, and 50 for a speed of 0.1 mm s^{-1}, to match the total energy fluence under different irradiation conditions. Table 1 summarizes the machining parameters and total energy fluence. Five lines were patterned for each condition. The sample was translated perpendicular to the cutting edge line, such that the focused beam was scanned over and out of the cutting edge line, as shown in Fig. 1.

2.2 Micro-cutting by the micropatterned diamond tool

The workpiece material was Ni, which was electroformed with a thickness of > 100 μm on SKD-61 substrate with ~10% phosphorus content; this is a commonly used mold material for plastic-film-forming processes. The patterned diamond tool was mounted to an ultra-precision machining system (UVM-450C, Toshiba) that had a positioning resolution of 10 nm along the X, Y, and Z axes, and an index resolution of 0.00001° along the rotation (R) axes. The diamond tool was mounted using a tool holder, which was supported by a force

Table 1 Machining parameters and total energy fluence

Translation speed (mm s^{-1})	Reciprocating number	Energy fluence (kJ cm^{-2})
0.01	1	28
	2	56
	5	140
0.05	1	5.6
	2	11.2
	5	28
0.1	10	28
	20	56
	50	140

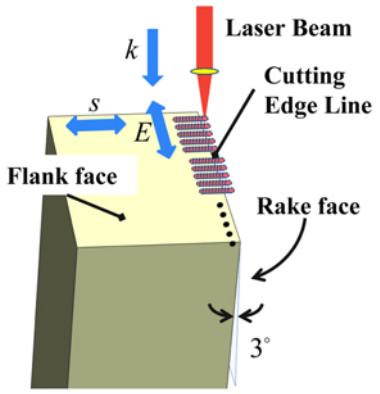

Fig. 1 Schematic diagram of a femtosecond laser micromachining on the surface of diamond. *k*, *E*, and *s* indicate the direction of the laser beam propagation, the electric field of the beam, and the sample motion, respectively

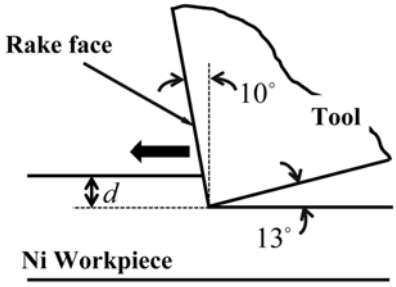

Fig. 2 Schematic diagram of diamond shaping of a Ni workpiece using a negative rake angle

dynamometer (9256C2, three-axis, piezoelectric, Kistler), and tilted 10° such that the rake angle was set to 10° with a clearance angle of 13° as shown in Fig. 2. Since the micropatterns on the flank face were formed 20 μm from the edge line, the clearance height at the end of the line was only about 1 μm with a rake angle of 0°. Therefore, a negative rake angle was used to prevent the micropattern formed by the edge line on the workpiece from pressing on the flank face as the diamond tool passed over.

In the preliminary cutting experiment, the Ni surface was cut to a depth of 3 μm under oil mist conditions, using a cutting speed of 100 mm s^{-1}. Scanning electron microscopy (SEM) and a confocal microscope were used to study the machined Ni surface.

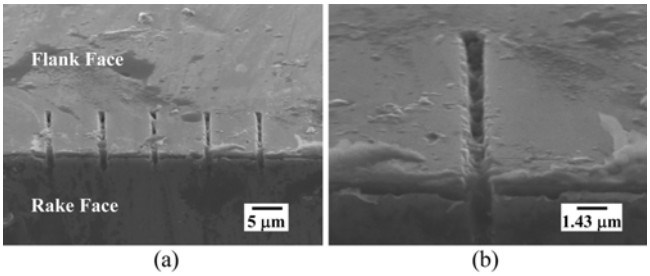

Fig. 3 (a) Scanning electron microscopy (SEM) image of the diamond tool edge, patterned with a reciprocal number of 5, using a translation speed of 0.01 mm s^{-1} (fluence: 140 kJ cm^{-2}), and (b) an enlarged image of (a)

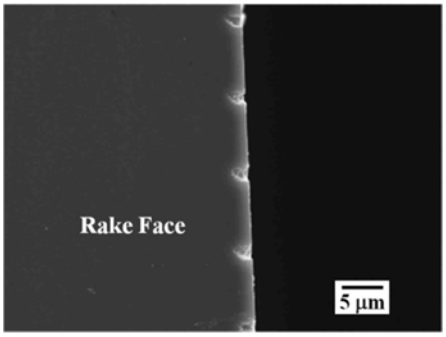

Fig. 4 SEM image of the diamond rake face, patterned with a reciprocal number of 1, using a translation speed of 0.05 mm s^{-1} (fluence: 5.6 kJ cm^{-2})

3. Results and Discussion

3.1 Femtosecond laser machining of bulk diamond

The total input fluence (E) is given by the following equation:

$$E = 2n\left(\frac{4 \times P}{\pi \times v \times D}\right)$$

where P is the laser power, D is the spot size, v is the translation speed, and n is the reciprocating number. Thus, reciprocal numbers of 1, 5, and 10 with speeds of 0.01, 0.05, and 0.1 mm s^{-1}, respectively, produced an input fluence of 28 kJ cm^{-2}. Reciprocal numbers of 5 and 50 with speeds of 0.01 and 0.1 mm s^{-1}, respectively, produced a fluence of 140 kJ cm^{-2} (refer to Table 1).

Fig. 3 shows an SEM image of the flank and rake face, patterned using a reciprocal number of 5 and translation speed of 0.01 mm s^{-1} (140 kJ cm^{-2}). Fig. 4 shows the flank face produced using a reciprocal number of 1 with a translation speed of 0.05 mm s^{-1} (5.6 kJ cm^{-2}). Although there was a slight difference in the machined depth, the outward appearance of the patterned diamond tool (Figs. 3 and 4) showed minimal thermal damage or cracking, despite the difference in energy fluence; this was an indication of nonthermal ablation. Moreover, the depth of the patterned groove was > 1 μm, which was much greater than the minimum uncut chip thickness expected (0.2~0.3 of the edge radius).[15] The cutting edge radius is estimated to be approximately in the range of 60~100 nm.[16] Therefore, the material could be removed without being ploughed.

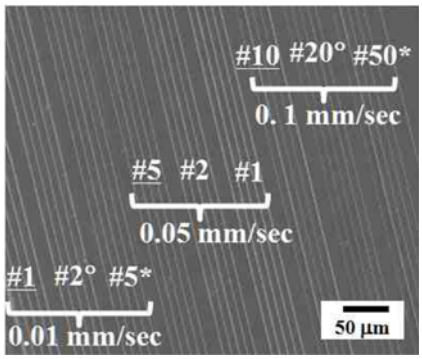

Fig. 5 SEM image of the micromachined pattern in Ni, created using the patterned diamond cutting tool. Three different translation speeds were used (0.01, 0.05, 0.1 mm s^{-1}) to create the pattern in the diamond tool. Areas of the pattern with the same input fluence are indicated by the same mark (underbar: 28 kJ cm^{-2}; circle: 56 kJ cm^{-2}; asterisk: 140 kJ cm^{-2})

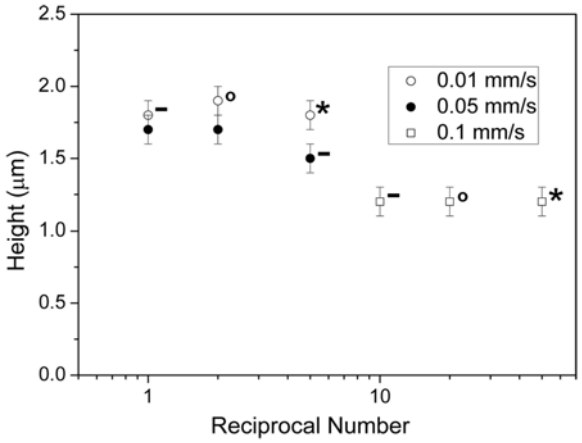

Fig. 6 Height comparison of the Ni surface obtained by the diamond tool patterned with different scanning translation speeds and reciprocal numbers. The same mark (underbar, circle, or asterisk) corresponds to the same fluence (refer to Fig. 5)

3.2 Machining of Ni using a micropatterned diamond cutting tool

The diamond tool was patterned using different scanning translation speeds and reciprocal numbers. This pattern was then cut into the Ni surface. Fig. 5 shows the entire Ni surface machined by the patterned diamond tool. Note that the entire pattern on Ni was machined with only a single pass of the diamond tool. The symbols by the reciprocal numbers (underbars, circles, and asterisks) in Fig. 5 indicate the same input fluence (used to create the pattern in the diamond tool); underbars correspond to a fluence of 28 kJ cm^{-2}, circles correspond to 56 kJ cm^{-2}, and asterisks to 140 kJ cm^{-2}. Fig. 6 shows the height of the pattern transferred from the diamond tool. The height of the features on the Ni surface was not significantly affected by the reciprocal number or total input fluence. Instead, translation speed appeared to have a greater influence on the feature height in the Ni.

The total fluence is much higher when the translation speed is slow. At the beginning of the machining process to create the pattern in the diamond tool, the surface of the diamond tool was clean enough to

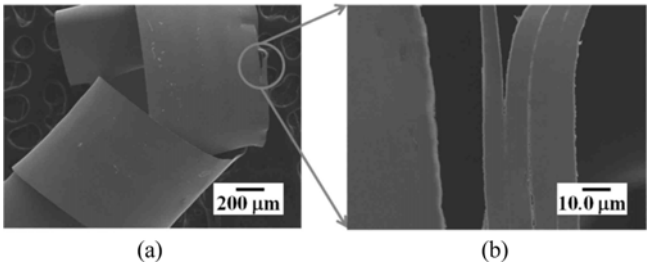

Fig. 7 SEM image of (a) a continuous chip, and (b) a magnified image of the split shown in (a)

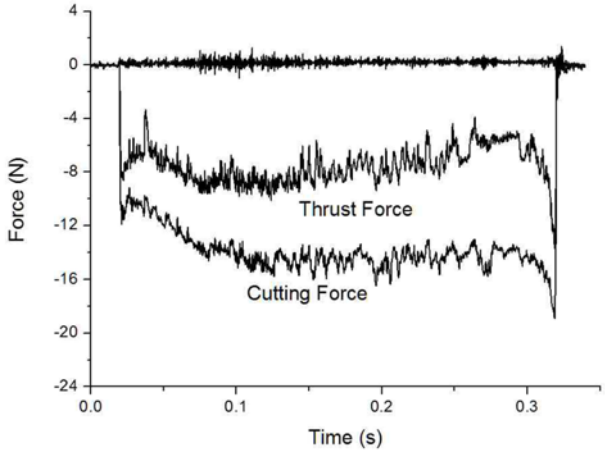

Fig. 8. Cutting and thrust force during shaping with a cutting depth of 3 μm, cutting speed of 100 mm s^{-1}, and a rake angle of -10°

absorb the laser energy. However, on the next pass, the laser beam was scattered considerably, due to the coarse roughness of the surface, thereby not reaching the ablation threshold. Moreover, due to the high NA of the objective lens, the depth of focus was too short, which increased the divergence of the beam. This may explain why the depth of the grooves in the diamond tool pattern was more affected by the translation speed in the first pass than the reciprocal number or total input fluence.

Fig. 7 shows a continuous chip of Ni obtained from the cutting experiment; a portion of the machined width was split. This may have been caused by the 1.8-μm groove depth in the diamond tool, formed with a reciprocal number of 1 using a translation speed of 0.01 mm s^{-1}. This value was close to the depth of the cut (3 μm) and positioned near the free side of the machined wall. The other parts of the Ni chip were clean.

Fig. 8 shows the cutting force monitored in real time during machining. The initial cutting force increased as the cutting length increased up to a certain point, and after that remained steady. The negative rake angle of 10° decreased the shear angle of the chip and increased the shear cross-section. This, in turn, increased the shear strain, thereby increasing the cutting force due to the friction between the rake face and the work surface. The absolute cutting force could be decreased by increasing the rake angle, which would be possible if the length of the lines patterned on the flank face of the diamond tool were longer.

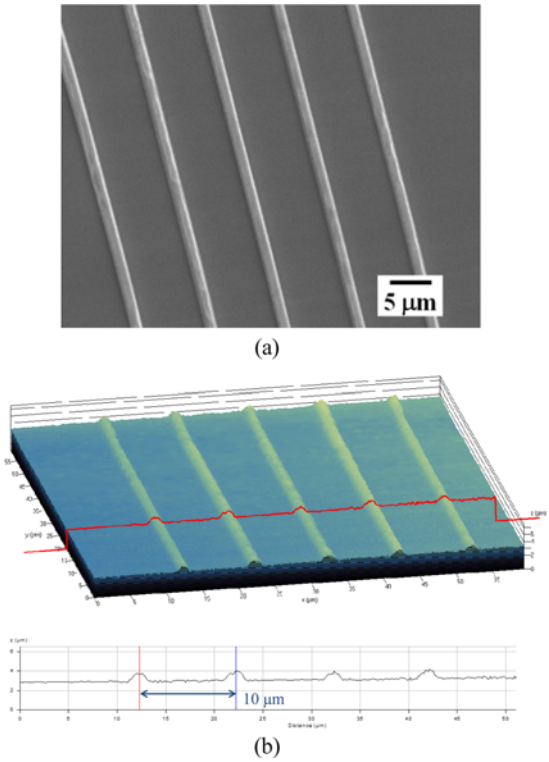

Fig. 9 (a) SEM image of multiple patterns in Ni, machined by a single pass of the patterned diamond cutting tool, and (b) corresponding heights of the pattern features

Fig. 9 shows a micropatterned Ni surface, produced using the patterned diamond cutting tool (translation speed: 0.05 m s^{-1}; reciprocal number: 5). A set of five lines was machined using the same cutting conditions; the lines exhibited uniform height and width. Although we demonstrated the patterned rectangular diamond cutting tool in this paper, this process can be applicable to the tool shape such as triangle, trapezoid and circle.

4. Conclusion

We demonstrated a novel technique for fabrication of multiple micropatterns on metal surfaces using a single pass of a patterned diamond cutting tool. In this study, we created a patterned rectangular diamond cutting tool using a 220-fs-pulsed Ti : Sapphire laser and a six-axis motion stage. The stage aligned the edge line and flank surface of the diamond tool with respect to the focal point of the laser beam to create a pattern along the 1-mm edge line of the diamond cutting tool. The pattern consisted of lines ~1.2 μm in width and 1.5~1.8 μm in depth. The depth of the grooves in the diamond tool pattern was significantly affected by the translation speed during pattern formation, due to beam scattering and divergence. The patterned diamond tool was then used to successfully create micropatterns on a Ni surface, using a single pass. The ability to obtain multiple micropatterns in a single-pass cut significantly decreases fabrication times and machining costs for micromachining of larger surface areas.

REFERENCES

1. Lee, Y. C., Chen, B. T., Wu, T. H., and Chou, Y. Y., "Full Wafer Microstructure Fabrication by Continuous UV-Assisted Roller Imprinting Lithography to Enhance Light Extraction of LEDs," Microelectronic Engineering, Vol. 91, pp. 64-69, 2012.
2. Sher, M. J., Winkler, M. T., and Mazur, E., "Pulsed-Laser Hyperdoping and Surface Texturing for Photovoltaics," MRS Bull, Vol. 36, No. 6, pp. 439-445, 2011.
3. Meng, F., Davis, T., Cao, J., Wang, Q. J., Hua, D., and Liu, J., "Study on Effect of Dimples on Friction of Parallel Surfaces under different Sliding Conditions," Applied Surface Science, Vol. 256, No. 9, pp. 2863-2875, 2010.
4. Costa, H. L. and Hutchings, I. M., "Effects of Die Surface Patterning on Lubrication in Strip Drawing," Journal of Materials Processing Technology, Vol. 209, No. 3, pp. 1175-1180, 2009.
5. Ramsden, J. J., Allen, D. M., Stephenson, D. J., Alcock, J. R., Peggs, G., and et al., "The Design and Manufacture of Biomedical Surfaces," CIRP Annals-Manufacturing Technology, Vol. 56, No. 2, pp. 687-711, 2007.
6. Cao, J., Yuan, W., Pei, Z., Davis, T., Cui, Y., and Beltran, M., "A Preliminary Study of the Effect of Surface Texture on Algae Cell Attachment for a Mechanical-Biological Energy Manufacturing System," Journal of Manufacturing Science and Engineering, Vol. 131, No. 6, Paper No. 064505, 2009.
7. Bruzzone, A. A. G., Costa, H. L., Lonardo, P. M., and Lucca, D. A., "Advances in Engineered Surfaces for Functional Performance," CIRP Annals-Manufacturing Technology, Vol. 57, No. 2, pp. 750-769, 2008.
8. Brinksmeier, E., Gläbe, R., and Schönemann, L., "Review on Diamond-Machining Processes for the Generation of Functional Surface Structures," CIRP Journal of Manufacturing Science and Technology, Vol. 5, No. 1, pp. 1-7, 2012.
9. Mao, S. S., Quéré, F., Guizard, S., Mao, X., Russo, R., and et al., "Dynamics of Femtosecond Laser Interactions with Dielectrics," Applied Physics A, Vol. 79, No. 7, pp. 1695-1709, 2004.
10. Gattass, R. R. and Mazur, E., "Femtosecond Laser Micromachining in Transparent Materials," Nature Photonics, Vol. 2, No. 4, pp. 219-225, 2008.
11. Shinoda, M., Gattass, R. R., and Mazur, E., "Femtosecond Laser-Induced Formation of Nanometer-Width Grooves on Synthetic Single-Crystal Diamond Surfaces," Journal of Applied Physics, Vol. 105, No. 5, Paper No. 053102, 2009.
12. Hsu, E. M., Mailman, N. A., Botton, G. A., and Haugen, H. K., "Microscopic Investigation of Single-Crystal Diamond Following Ultrafast Laser Irradiation," Applied Physics A, Vol. 103, No. 1, pp. 185-192, 2011.
13. Pettersson, U. and Jacobson, S., "Tribological Texturing of Steel Surfaces with a Novel Diamond Embossing Tool Technique," Tribology International, Vol. 39, No. 7, pp. 695-700, 2006.
14. Kuang, Z., Liu, D., Perrie, W., Edwardson, S., Sharp, M., and et al., "Fast Parallel Diffractive Multi-Beam Femtosecond Laser Surface Micro-Structuring," Applied Surface Science, Vol. 255, No. 13, pp. 6582-6588, 2009.
15. Malekian, M., Mostofa, M., Park, S., and Jun, M., "Modeling of Minimum Uncut Chip Thickness in Micro Machining of Aluminum," Journal of Materials Processing Technology, Vol. 212, No. 3, pp. 553-559, 2012.
16. Ng, C. K., Melkote, S. N., Rahman, M., and Senthil Kumar, A., "Experimental Study of Micro-and Nano-Scale Cutting of Aluminum 7075-T6," International Journal of Machine Tools and Manufacture, Vol. 46, No. 9, pp. 929-936, 2006.